

Supplemental Information for

Oleic acid differentially affects lipid droplet storage of *de novo* synthesized lipids in adipocytes and hepatocytes

Hannah B. Castillo, Sydney O. Shuster, Lydia H. Tarekegn and Caitlin M. Davis

Contents

Experimental Methods

- Materials
- Oleic acid conjugation and feeding protocol
- Huh-7 cell culture and ^{13}C and ^2H labeling
- Differentiated 3T3-L1 cell culture and ^{13}C and ^2H labeling
- Cell fixing
- Live cell chamber construction
- OPTIR data collection
- Data analysis
- Lipid droplet size analysis
- Presentation of results and statistics

Supplemental Figures

- Figure S1. Spatial resolution of OPTIR
- Figure S2. Full assignments of a ^{12}C glucose fed cell and ^{13}C glucose and ^2H OA fed cells
- Figure S3. Full assignments of ^2H oleic acid spectrum and cell fed with probes
- Figure S4. Sensitivity limit of OPTIR
- Figure S5. Live Huh-7 cell after 72 hours of feeding ^{13}C glucose
- Figure S6. Line scan across a lipid droplet
- Figure S7. Visualization of rates of *de novo* lipid storage in live differentiated 3T3-L1
- Figure S8. Visualization of rates of *de novo* lipid storage in fixed Huh-7 cells
- Figure S9. Visualization of rates of *de novo* lipid storage in fixed differentiated 3T3-L1
- Figure S10. Fixed cell rates of ^{13}C incorporation in the vehicle and ^2H oleic acid
- Figure S11. Lipid droplet comparison brightfield images
- Figure S12. Slopes of ^{13}C incorporation rates
- Figure S13. Spectra based image correction

Supplemental Tables

- Table S1: Average ratios of live and fixed Huh-7 cells fed with ^2H OA and ^{13}C glucose
- Table S2: Average ratios of live and fixed Huh-7 cells fed with ^{13}C glucose in BSA
- Table S5: Average ratios of live and fixed adipocytes fed with ^2H OA and ^{13}C glucose
- Table S6: Average ratios of live and fixed adipocytes fed with ^2H OA in BSA
- Note: Tables S3, S4, S7, S8, and S9 are found in the attached excel files.

References

Experimental Methods

Materials

Unless otherwise specified, all reagents were sourced from Sigma-Aldrich.

Oleic Acid Conjugation and Feeding Protocol

For feeding, ^2H oleic acid (oleic acid- d_{33} , DLM-1891-PK, Cambridge Isotope Laboratories, Tewksbury, MA) was bound to fatty acid-free bovine serum albumin (BSA) using a protocol from Shi et al.¹ In a 2 mL clear glass container (VWR, Radnor, PA), Milli-Q purified water, 20 μL of 1 M NaOH, and 2.3 μL of ^2H oleic acid were combined and heated in a 70 °C water bath until clear. A solution of 150 mg/mL fatty acid-free bovine serum albumin (BSA) was then added to the ^2H oleic acid solution and heated again at 37 °C in a water bath until clear. The solution was then filtered with a 0.2 μm filter into another 2 mL clear glass container. The stock oleic acid concentration is approximately 3 mM. The ratio of oleic acid to BSA is 2:1, in line with physiological ratios.^{2,3} Oleic acid is then incubated with cell culture at a concentration of 60 μM , within a physiologically relevant range of oleic acid in human plasma⁴ and less than the total fatty acid content in 10% FBS supplemented cell culture media.⁵ Free OA is likely much lower than 60 μM as most will remain bound to BSA.²

Huh-7 cell culture and ^{13}C and ^2H labeling

Huh-7 cells (gift from Lars Plate, Vanderbilt University) were cultured in 75 cm^3 sterile vented cap tissue culture flasks (Corning, Corning, NY). Cells were grown to 80 % confluence in Dulbecco's modified Eagle's medium containing 4.5 g/L glucose and L-glutamine (DMEM, Corning) supplemented with 10% fetal bovine serum (FBS) and 1% penicillin/streptomycin (Thermo-Fischer, Waltham, MA) under standard conditions (37° C, humidified atmosphere, 5% CO_2). At 80 % confluence, cells were trypsinized and replated on CaF_2 coverslips (20 x 20 x 0.35 mm, Crystran, Poole, U.K.) in 35 mm diameter sterile Petri dishes (Corning) for live samples and CaF_2 coverslips (10 x 10 x 0.35 mm) in a 24 well cell culture plate (Corning) for fixed samples. After a day of allowing cells to adhere to the coverslips, the media was replaced with glucose-free DMEM supplemented with 1% FBS, 1% penicillin/streptomycin, ^{13}C glucose (D-glucose- $^{13}\text{C}_6$, CLM-1396-PK, Cambridge Isotope Laboratories) to 4.5 mg/mL, and either 2% BSA or 2% ^2H oleic acid conjugated with BSA (final concentration 60 μM OA and 30 μM BSA).

Differentiated 3T3-L1 cell culture and ^{13}C and ^2H labeling

3T3-L1 cells (ATCC, Manassas, VA) were prepared as previously described.⁶ Briefly, low passage number (<10), pre-differentiated cells were grown to confluence in Dulbecco's modified Eagle's medium containing 4.5 g/L glucose and L-glutamine (DMEM, Corning) supplemented with 10% calf bovine serum (CBS, ATCC) and 1% penicillin/streptomycin (Thermo-Fischer) under standard conditions. Two to three days post confluence, media was changed to DMEM containing 10% fetal bovine serum (FBS, Corning), 1% penicillin/streptomycin, 20 $\mu\text{g}/\text{mL}$ insulin, 250 nM dexamethasone, and 500 μM isobutylmethylxanthine. Two to three days after differentiation, media was changed to DMEM containing 10% fetal bovine serum (FBS, Corning), 1% penicillin/streptomycin and 20 $\mu\text{g}/\text{mL}$ insulin. After 2-3 days, cells were trypsinized and replated on CaF_2 coverslips (20 x 20 x 0.35 mm; Crystran.) in 50 mm dishes (Corning). Media was exchanged every 2-3 days until lipid droplets formed and stabilized (5-7 days). At this point, medium was changed to glucose-free DMEM supplemented with 1% FBS, 1%

penicillin/streptomycin, ^{13}C - labeled glucose to 4.5 mg/mL, and either 2% BSA or 2% ^2H oleic acid conjugated with BSA (final concentration 60 μM OA and 30 μM BSA).

Cell fixing

For fixed cell samples, both cell lines were fixed at the desired time points with 4% paraformaldehyde (PFA) in PBS (Corning) for 20 minutes at room temperature and washed three times with PBS followed by three times with Milli-Q purified water and allowed to air-dry before analysis.

Live cell chamber construction

After feeding, live cell samples from both cell lines were washed once with PBS and mounted in PBS on a glass microscopy slide (VWR) with double-sided tape spacers (Nitto, San Diego, CA) with a 5 μm thickness to keep the cells hydrated and sealed and minimize compression of the cell.

OPTIR data collection

All imaging was performed on a mIRage-LS IR microscope (Photothermal Spectroscopy Corporation, Santa Barbara, CA) integrated with a four-module-pulsed quantum cascade laser (QCL) system (Daylight Solutions, San Diego, CA) with a tunable range from 932 cm^{-1} to 2348 cm^{-1} . Brightfield optical images were collected using a low magnification 10X refractive objective with a working distance of 15 mm. Spectra and infrared images were collected in co-propagating mode using a 40X Cassegrain objective with a working distance of 8 mm. Fixed cell spectra and images were collected in standard (reflective) mode and live cell spectra and images were collected in transmission mode. Data was collected with an IR laser power of 20 % and a probe power in the range of 5-11 %. All spectra and images were collected using PTIR Studio 4.5. (Photothermal Spectroscopy Corporation). Image acquisition time was 2-5 minutes per frequency for a total acquisition time of 10-25 minutes per cell.

Data analysis

Images were processed in Fiji (NIH, Bethesda, MD).⁷ Spectra were analyzed in Igor Pro 9 (Wavemetrics, Portland, OR). Live and fixed cell ratio images were generated in Python 3.10 in Colab (Google, Mountain View, CA).⁸

Ratio images must be corrected to account for overlapping signals of other biomolecules (Figure S13). This is done through a correction protocol adapted⁶ from Shi et al.,¹ which removes contribution from the water band and protein amide I. Correction values are calculated for each cell line after analyzing single cell spectra in which no lipid signal is present. The intensity at the wavenumber at which lipid signal is collected (either $^{13}\text{C}=\text{O}$, $^{12}\text{C}=\text{O}$, or $^{12}\text{C}-^2\text{H}$) is divided by the intensity at the amide I (1655 cm^{-1}) or water band (2050 cm^{-1}). These values are collected per cell across all time points and averaged to create a correction value with which to subtract off overlapping amide-I and water intensity for lipid intensities.

Fixed cell $^{13}\text{C}=\text{O}/^{12}\text{C}=\text{O}$ ratio images were corrected for the amide-I intensity using equation 1:

$$\frac{^{13}\text{C}}{^{12}\text{C}} \text{ ester carbonyl intensity} = \frac{A_{^{13}\text{C}=\text{O}} - bA_{\text{Amide I}}}{A_{^{12}\text{C}=\text{O}}} \quad \text{Equation 1}$$

Where A is the signal intensity of the frequency of the indicated biomolecule. The $^{12}\text{C}=\text{O}$ stretch is at 1744 cm^{-1} for Huh-7 cells and at 1747 cm^{-1} for adipocytes. For both cell lines, the $^{13}\text{C}=\text{O}$ stretch is at 1703 cm^{-1} . The variable b is the correction value for the amide-I intensity, with b being 0.34 for Huh-7 cells and 0.31 for adipocytes. There was no correction done for fixed $^2\text{H}\text{-C}/^{12}\text{C}=\text{O}$ ratio images. Fixed cell ratios were only performed on regions with sufficient $^{12}\text{C}=\text{O}$ signal intensity, defined as regions with 15% of the maximum value of $^{12}\text{C}=\text{O}$ signal for Huh-7 cells and 5% for adipocytes which visually corresponded to the lipid rich areas of the cells as determined by examining the single wavenumber images at 1744 cm^{-1} and the brightfield view of lipid droplets.

Live cell $^{13}\text{C}=\text{O}/^{12}\text{C}=\text{O}$ ratio images were corrected for the amide I and water band intensity using equation 2.

$$\frac{^{13}\text{C}}{^{12}\text{C}} \text{ ester carbonyl intensity} = \frac{A_{^{13}\text{C}=\text{O}} - cA_{\text{Amide I}}}{A_{^{12}\text{C}=\text{O}} - dA_{\text{Amide I}}} \quad \text{Equation 2}$$

Where c is the correction value for $A_{^{13}\text{C}=\text{O}}$ and is 0.61 for Huh-7 cells and 0.66 for adipocytes and d is the correction value for $A_{^{12}\text{C}=\text{O}}$ and is 0.31 for Huh-7 cells and 0.28 for adipocytes. Live cell $^2\text{H}/^{12}\text{C}$ ratio images were corrected for the water band using equation 3.

$$\frac{^2\text{H}}{^{12}\text{C}} \text{ ester carbonyl intensity} = \frac{A_{^{12}\text{C}-^2\text{H}} - fA_{\text{water band}}}{A_{^{12}\text{C}=\text{O}} - dA_{\text{Amide I}}} \quad \text{Equation 3}$$

The $^{12}\text{C}-^2\text{H}$ is measure from a shoulder at 2214 cm^{-1} for Huh-7 cells and at 2212 cm^{-1} for adipocytes. The water band is measured from 2050 cm^{-1} for both cell lines as this does not overlap with other $^{12}\text{C}-^2\text{H}$ stretches. The variable f is the correction value for the water band and is 0.87 for Huh-7 cells and 0.85 for adipocytes and d is the correction value discussed above. Live cell ratios were also only performed on regions with sufficient ^{12}C lipid ester carbonyl signal intensity, defined as regions with 15% of the maximum value of ^{12}C lipid ester carbonyl signal for Huh-7 cells and 5 % for adipocytes.

Lipid droplet size analysis

Lipid droplet size and diameter were determined using Fiji on cells at 48 hours after feeding with ^{13}C glucose and either ^2H oleic acid or BSA. The number of lipid droplets per cell were counted and the size of each lipid droplet determined using the line tool and measuring the diameter. These values were averaged over a total of 30 cells for both ^2H oleic acid fed and BSA fed trials.

Presentation of results and statistics

Calculations for averages and statistical analysis were performed in Microsoft Excel (Microsoft, Redmond, WA). Bar graphs were generated by averaging the average ratios of N cells (Tables S1-8) at each time point. Error bars represent one standard deviation of average of the averages of the cells at each time point including propagated error from the standard error of each cell. Two tailed student's t-tests were performed in Excel to determine significance between time points in trials.

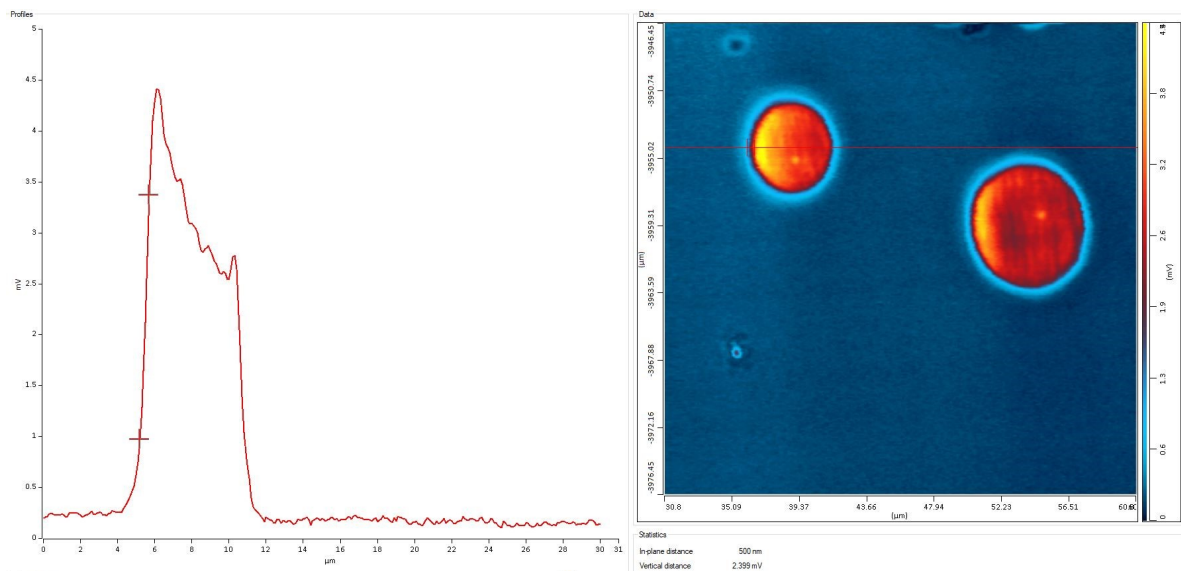


Figure S1. Instrument resolution. Profile line (left) and full image (right) of 1720 cm^{-1} intensity of section of PMMA beads embedded in epoxy. Beads are resolved from the background at a resolution of 500 nm or less (in-plane distance). The authors acknowledge Photothermal Spectroscopy Inc as this data was collected during instrument install.

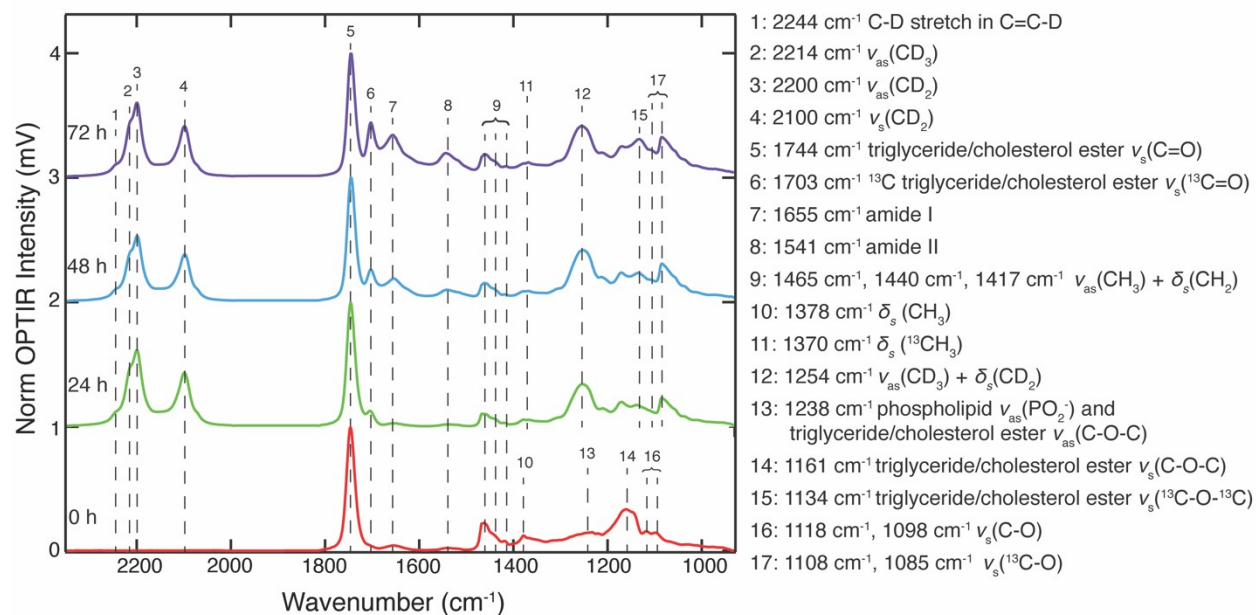
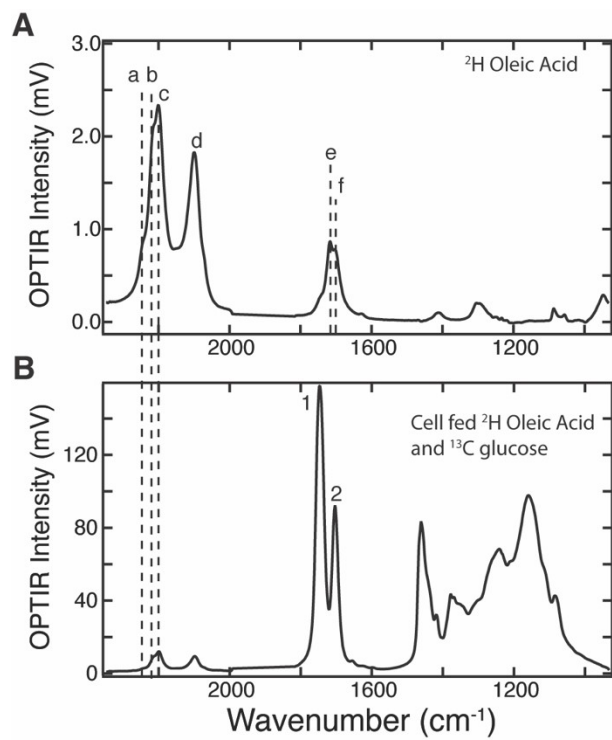


Figure S2: Full assignments of a representative fixed Huh-7 cell fed ¹²C glucose (0 hour, red) and after 24 (green), 48 (blue), and 72 (purple) hours of ¹³C glucose and ²H oleic acid feeding.^{6,9-11}



- a = 2246 cm^{-1} ambiguous C-D stretch in C=C-D
- b = 2214 cm^{-1} ambiguous C-D stretch in C=C-D
- c = $2200 \text{ cm}^{-1} \nu_{\text{as}}(\text{CD}_2)$
- d = $2098 \text{ cm}^{-1} \nu_{\text{s}}(\text{CD}_2)$
- e = $1716 \text{ cm}^{-1} \nu_{\text{s}}(\text{C}=\text{O}$ free fatty acid)
- 1 = $1744 \text{ cm}^{-1} \nu_{\text{s}}(\text{C}=\text{O}$ triglyceride)
- 2 = $1703 \text{ cm}^{-1} \nu_{\text{s}}(^{13}\text{C}=\text{O}$ triglyceride)

Figure S3: Full assignments of (A) ^2H oleic acid IR spectrum^{9,11} and (B) a live differentiated 3T3-L1 cell 72 hours after feeding with ^2H oleic acid and ^{13}C glucose.

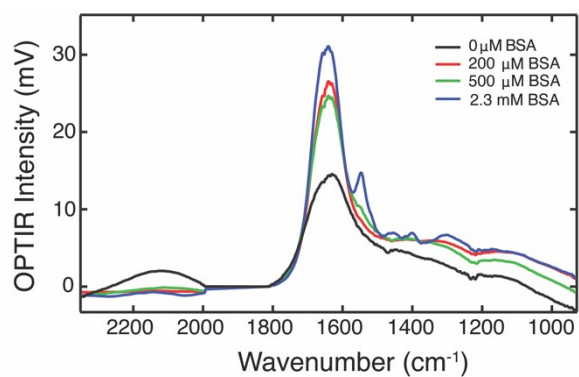


Figure S4: Detection limit of the OPTIR determined by comparing the spectra of 0, 0.2, 0.5, and 2.3 mM bovine serum albumin (BSA).

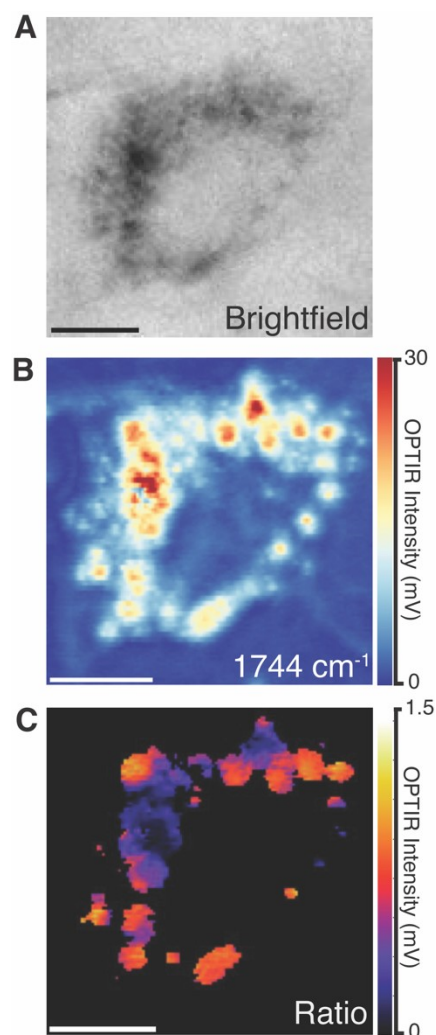


Figure S5: Rates of *de novo* lipid storage in live Huh-7 cells can be observed by OPTIR imaging approach previously used on adipocytes. (A) Brightfield image of a ¹³C glucose-fed Huh-7 cell at 72 hours. (B) Single wavenumber image collected at the ¹²C=O lipid band (1744 cm⁻¹) and (C) the corresponding ratio image of ¹³C=O lipid ester carbonyl of triglycerides to ¹²C=O lipid band, after correction. Scale bars are 10 μm.

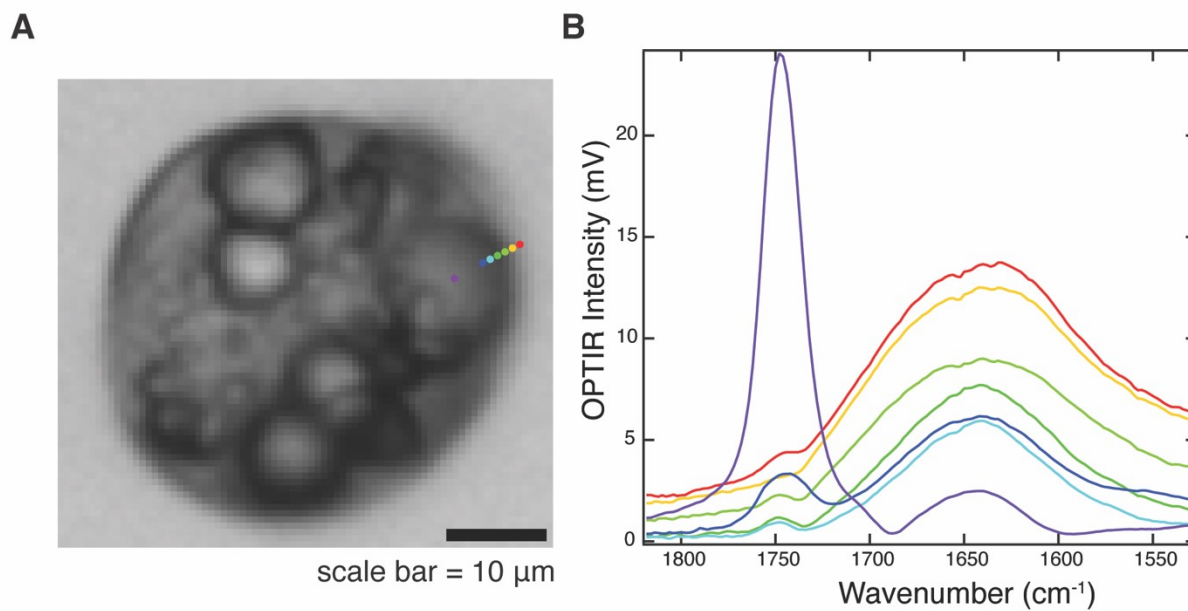


Figure S6. Spatial resolution of OPTIR. (A) Brightfield image of live 3T3-L1 cell with points indicating where spectra (B) were collected. 500 nm separate each point except for the purple spectrum at the center of the droplet.

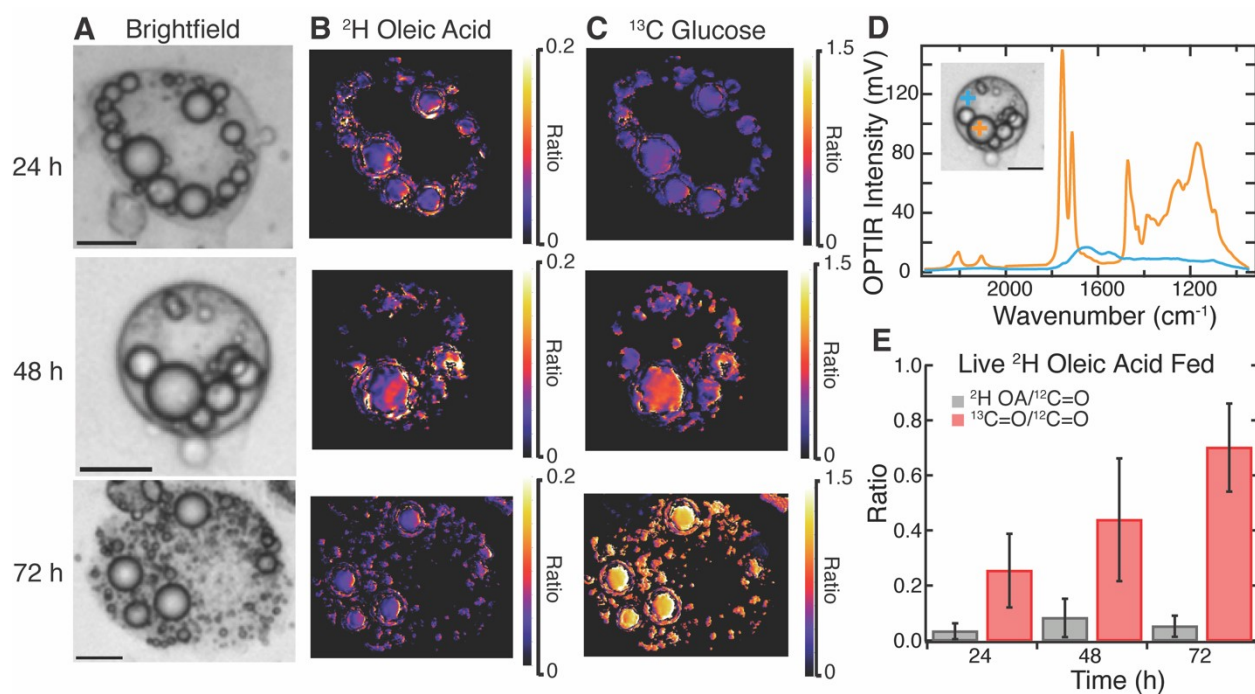


Figure S7: Visualization of rates of *de novo* lipid storage in live differentiated 3T3-L1 cells fed with both deuterated oleic acid and ^{13}C glucose for 24 to 72 h. (A) Brightfields images of live cells. (B) ^2H OA ratio images of ^2H lipid to the ^{12}C lipid band, after correction. (C) ^{13}C glucose ratio images of the ^{13}C lipid band to the ^{12}C lipid band, after correction. Scale bars are 10 μm . (D) A representative spectra of the live differentiated 3T3-L1 cell at the 48-hour time point. Orange trace was collected in a lipid droplet while blue was collected outside the droplet. (E) Average ratios of ^2H lipid band (grey) and ^{13}C lipid band (red) to ^{12}C lipid band across many cells $N=7-11$ cells per time point.

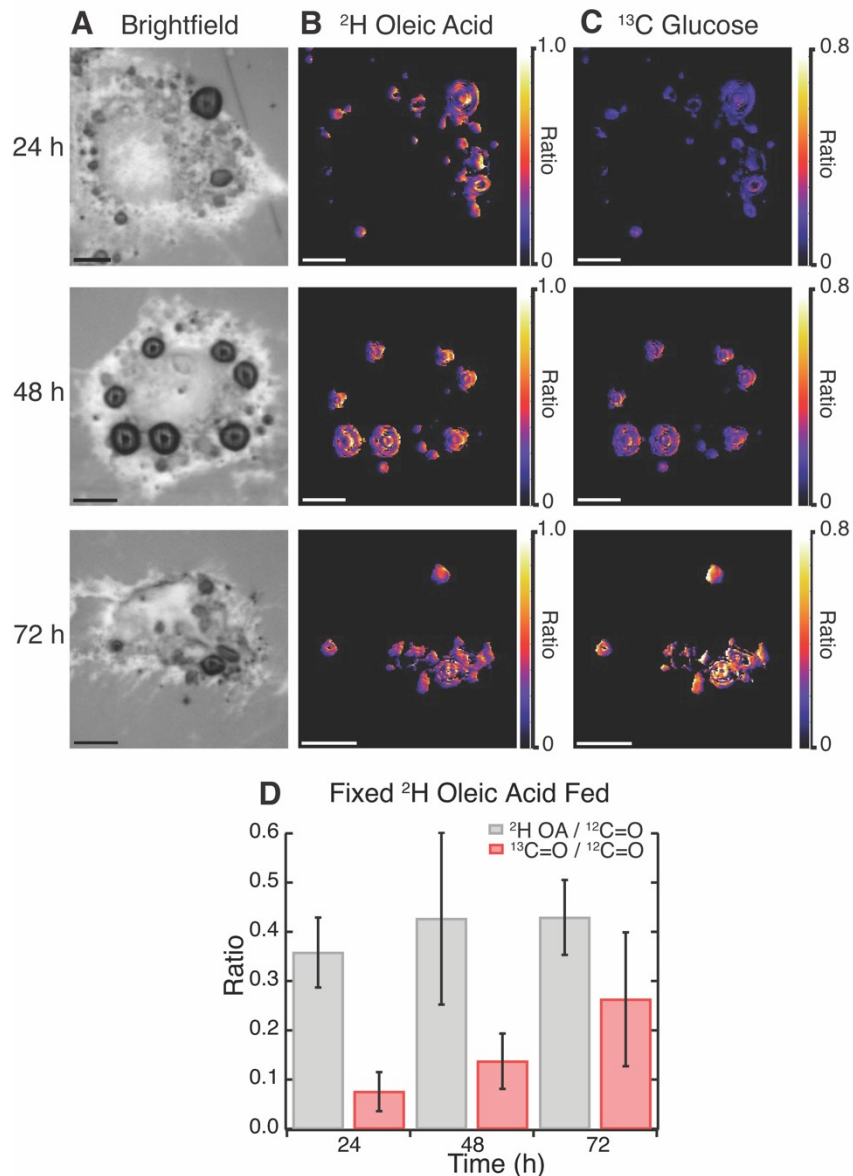


Figure S8: Visualization of rates of *de novo* lipid storage in fixed Huh-7 cells after feeding of ^2H oleic acid and ^{13}C glucose for 24-72 h. (A) Brightfield images of fixed Huh-7 cells (B) ^2H OA ratio images of ^2H lipid to the ^{12}C lipid band, after correction. (C) ^{13}C glucose ratio images of the ^{13}C lipid band to the ^{12}C lipid band, after correction. Scale bars are 10 μm . (D) Average ratios of ^2H lipid band (grey) and ^{13}C lipid band (red) to ^{12}C lipid band across many cells. N=12-16 cells per time point.

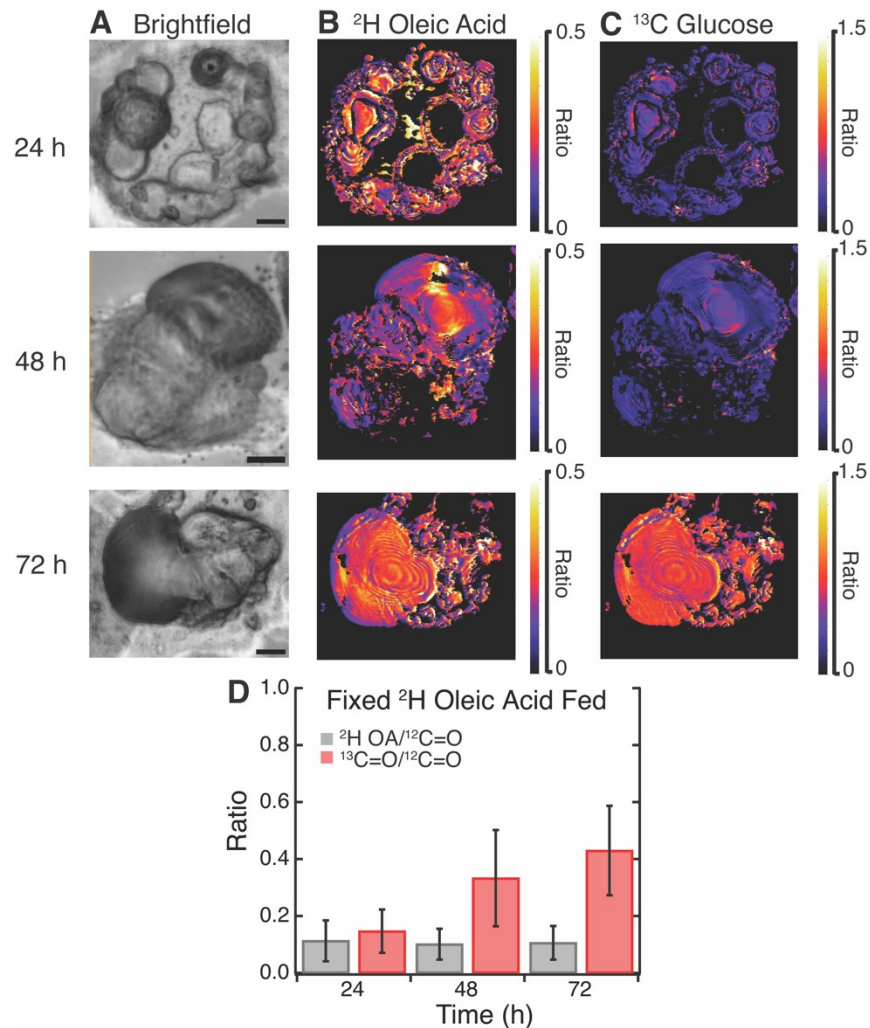


Figure S9: Visualization of rates of *de novo* lipid storage in fixed differentiated 3T3-L1 cells after feeding of ^2H oleic acid and ^{13}C glucose for 24-72 h. (A) Brightfields of fixed differentiated 3T3-L1 cells. (B) ^2H OA ratio images of ^2H lipid to the ^{12}C lipid band, after correction. (C) ^{13}C glucose ratio images of the ^{13}C lipid band to the ^{12}C lipid band, after correction. Scale bars are 10 μm . (D) Average ratios of ^2H lipid band (grey) and ^{13}C lipid band (red) to ^{12}C lipid band across many cells. N=11-13 cells per time point.

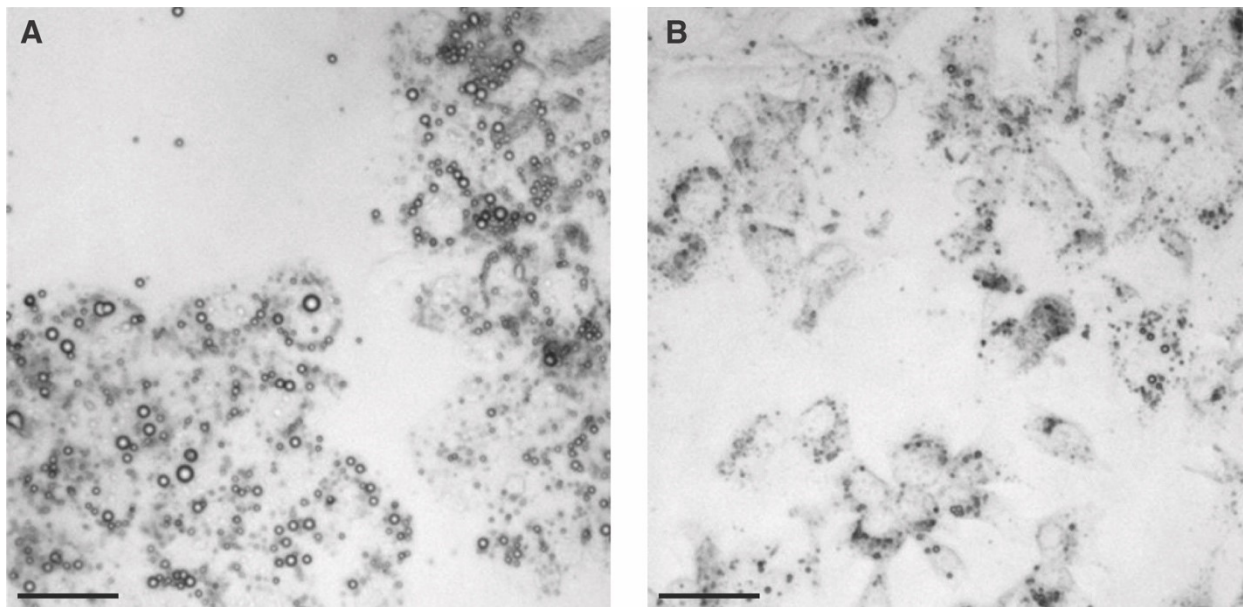


Figure S10: Lipid droplet comparison in Huh-7 cells at 48 hours after (A) feeding with ^2H oleic acid and ^{13}C glucose and (B) feeding with BSA and ^{13}C glucose. Scale bars are 50 μm .

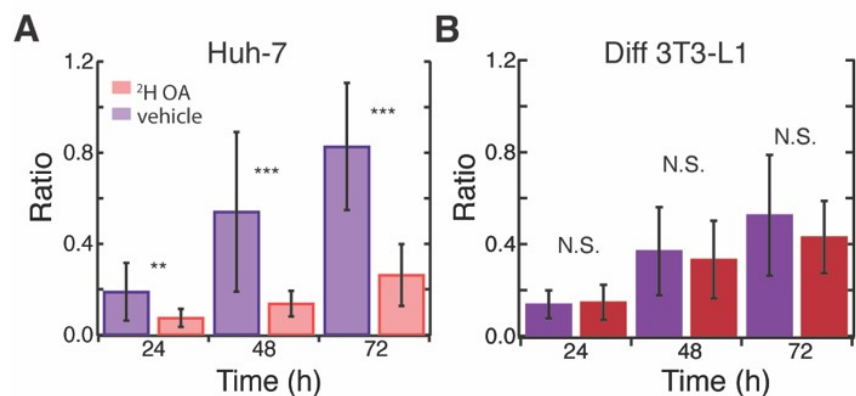


Figure S11: Effect of OA feeding on *de novo* lipid storage in fixed cells. Rates of uptake of ¹³C glucose in ²H OA trials (red) compared to in the BSA vehicle (purple) show that oleic acid has different effects between (A) fixed Huh-7 cells and (B) fixed differentiated 3T3-L1 cells. N= 7-16 cells per time point. * p-value< 0.05, ** p-value<0.005, ***p-value<0.0005

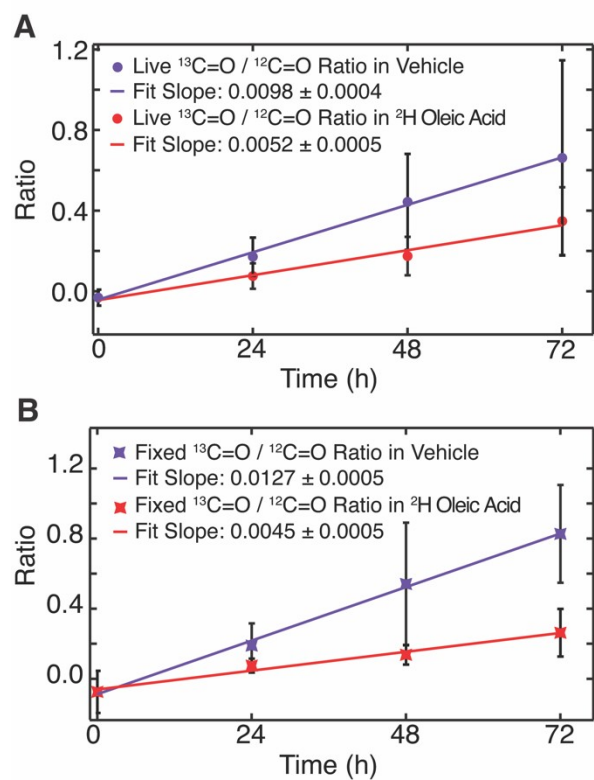


Figure S12: Slopes of the linear fit of $^{13}\text{C}=\text{O}$ to $^{12}\text{C}=\text{O}$ ratios in the vehicle and oleic acid at respective time points in (A) live and (B) fixed Huh-7 cells support the observation of a suppression of *de novo* lipid storage with exposure to oleic acid.

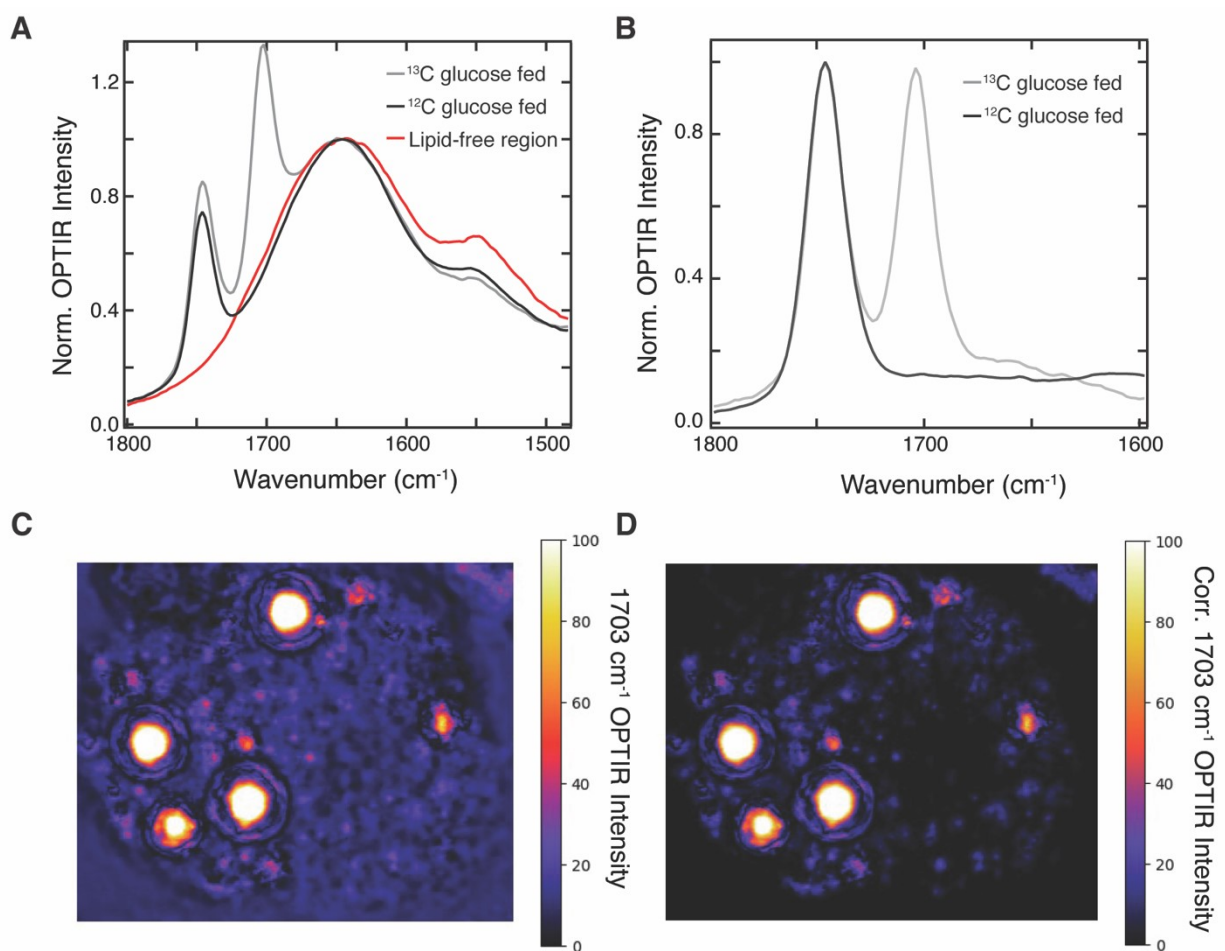


Figure S13. Spectra based image correction. Representative spectra collected in small (A) and large (B) lipid droplets of ^{12}C glucose (black) and ^{13}C glucose (grey) fed living adipocyte cells. Representative spectra of water and amide I background collected in lipid free region of ^{13}C glucose fed cell (red). Spectra are normalized at 1650 cm^{-1} . Image of a living adipocyte at 1703 cm^{-1} before (C) and after (D) correction for interference from protein and water.

Table S1: Average ratios of live and fixed Huh-7 cells fed with ^2H OA and ^{13}C glucose.

Table S2: Average ratios of live and fixed Huh-7 cells fed with ^{13}C glucose in vehicle (BSA).

<i>Live</i>			
Hour	N	Avg $^2\text{H OA} / ^{12}\text{C=O}$	Avg $^{13}\text{C=O} / ^{12}\text{C=O}$
24	14	0.19 ± 0.07	0.08 ± 0.06
48	14	0.18 ± 0.08	0.17 ± 0.10
72	14	0.17 ± 0.07	0.4 ± 0.2
<i>Fixed</i>			
Hour	N	Avg $^2\text{H OA} / ^{12}\text{C=O}$	Avg $^{13}\text{C=O} / ^{12}\text{C=O}$
24	12	0.36 ± 0.07	0.08 ± 0.04
48	16	0.4 ± 0.2	0.14 ± 0.06
72	16	0.39 ± 0.08	0.3 ± 0.1

<i>Live</i>		
Hour	N	Avg $^{13}\text{C=O} / ^{12}\text{C=O}$
24	12	0.2 ± 0.1
48	12	0.4 ± 0.2
72	11	0.7 ± 0.5
<i>Fixed</i>		
Hour	N	Avg $^{13}\text{C=O} / ^{12}\text{C=O}$
24	12	0.2 ± 0.1
48	16	0.5 ± 0.4
72	16	0.8 ± 0.3

Table S5: Average ratios of live and fixed differentiated 3T3-L1 cells fed with ^2H OA and ^{13}C glucose.

<i>Live</i>			
Hour	N	Avg ^2H OA / $^{12}\text{C}=\text{O}$	Avg $^{13}\text{C}=\text{O}/^{12}\text{C}=\text{O}$
24	7	0.03 ± 0.03	0.3 ± 0.1
48	7	0.09 ± 0.07	0.5 ± 0.2
72	11	0.05 ± 0.04	0.7 ± 0.2
<i>Fixed</i>			
Hour	N	Avg ^2H OA / $^{12}\text{C}=\text{O}$	Avg $^{13}\text{C}=\text{O}/^{12}\text{C}=\text{O}$
24	11	0.11 ± 0.07	0.15 ± 0.08
48	11	0.10 ± 0.05	0.3 ± 0.2
72	13	0.11 ± 0.06	0.4 ± 0.2

Table S6: Average ratios of live and fixed differentiated 3T3-L1 cells fed with ^{13}C glucose in vehicle (BSA).

<i>Live</i>		
Hour	N	Avg $^{13}\text{C}=\text{O}/^{12}\text{C}=\text{O}$
24	8	0.36 ± 0.09
48	8	0.6 ± 0.2
72	10	0.6 ± 0.2
<i>Fixed</i>		
Hour	N	Avg $^{13}\text{C}=\text{O}/^{12}\text{C}=\text{O}$
24	8	0.14 ± 0.06
48	9	0.4 ± 0.2
72	9	0.5 ± 0.3

References

- (1) Shi, L.; Liu, X.; Shi, L.; Stinson, H. T.; Rowlette, J.; Kahl, L. J.; Evans, C. R.; Zheng, C.; Dietrich, L. E. P.; Min, W. Mid-Infrared Metabolic Imaging with Vibrational Probes. *Nat. Methods* **2020**, *17* (8), 844–851. <https://doi.org/10.1038/s41592-020-0883-z>.
- (2) Alsabeeh, N.; Chausse, B.; Kakimoto, P. A.; Kowaltowski, A. J.; Shirihai, O. Cell Culture Models of Fatty Acid Overload: Problems and Solutions. *Biochim. Biophys. Acta* **2018**, *1863* (2), 143–151. <https://doi.org/10.1016/j.bbali.2017.11.006>.
- (3) Kleinfeld, A. M.; Prothro, D.; Brown, D. L.; Davis, R. C.; Richieri, G. V.; DeMaria, A. Increases in Serum Unbound Free Fatty Acid Levels Following Coronary Angioplasty. *Am. J. Cardiol.* **1996**, *78* (12), 1350–1354. [https://doi.org/10.1016/S0002-9149\(96\)00651-0](https://doi.org/10.1016/S0002-9149(96)00651-0).
- (4) Abdelmagid, S. A.; Clarke, S. E.; Nielsen, D. E.; Badawi, A.; El-Sohemy, A.; Mutch, D. M.; Ma, D. W. L. Comprehensive Profiling of Plasma Fatty Acid Concentrations in Young Healthy Canadian Adults. *PLoS ONE* **2015**, *10* (2), e0116195. <https://doi.org/10.1371/journal.pone.0116195>.
- (5) Else, P. L. The Highly Unnatural Fatty Acid Profile of Cells in Culture. *Prog. Lipid Res.* **2020**, *77*, 101017. <https://doi.org/10.1016/j.plipres.2019.101017>.
- (6) Shuster, S. O.; Burke, M. J.; Davis, C. M. Spatiotemporal Heterogeneity of De Novo Lipogenesis in Fixed and Living Single Cells. *J. Phys. Chem. B* **2023**, *127* (13), 2918–2926. <https://doi.org/10.1021/acs.jpcc.2c08812>.
- (7) Schindelin, J.; Arganda-Carreras, I.; Frise, E.; Kaynig, V.; Longair, M.; Pietzsch, T.; Preibisch, S.; Rueden, C.; Saalfeld, S.; Schmid, B.; Tinevez, J.-Y.; White, D. J.; Hartenstein, V.; Eliceiri, K.; Tomancak, P.; Cardona, A. Fiji: An Open-Source Platform for Biological-Image Analysis. *Nat. Methods* **2012**, *9* (7), 676–682. <https://doi.org/10.1038/nmeth.2019>.
- (8) Van Rossum, G.; Drake, F. L. *Python 3 Reference Manual*; CreateSpace: Scotts Valley, CA, 2009.
- (9) Yamawaki, H.; Fujihisa, H. Infrared Spectra of the β and γ Phases of Oleic Acid under High Pressure. *Spectrochim. Acta. A. Mol. Biomol. Spectrosc.* **2022**, *265*, 120290. <https://doi.org/10.1016/j.saa.2021.120290>.
- (10) Barth, A. Infrared Spectroscopy of Proteins. *Biochim. Biophys. Acta BBA - Bioenerg.* **2007**, *1767* (9), 1073–1101. <https://doi.org/10.1016/j.bbabi.2007.06.004>.
- (11) Hsi, S. C.; Tulloch, A. P.; Mantsch, H. H.; Cameron, D. G. A Vibrational Study of the CD₂ Stretching Bands of Selectively Deuterated Palmitic and Stearic Acids. *Chem. Phys. Lipids* **1982**, *31* (1), 97–103. [https://doi.org/10.1016/0009-3084\(82\)90022-6](https://doi.org/10.1016/0009-3084(82)90022-6).